coatings

MDPI

Article

Hybrid Ti-MoS_2 Coatings for Dry Machining of Aluminium Alloys

Tomasz L. Brzezinka [1], Jeff Rao [1], Mohamad Chowdhury [2], Joern Kohlscheen [3], German S. Fox Rabinovich [2], Stephen C. Veldhuis [2] and Jose L. Endrino [1,*]

1 Surface Engineering and Nanotechnology Institute (SENTi), Cranfield University, Cranfield MK43 0AL, UK; t.l.brzezinka@cranfield.ac.uk (T.L.B.); J.Rao@cranfield.ac.uk (J.R.)
2 Department of Mechanical Engineering, McMaster University, 1280 Main St. W., Hamilton, ON L8S4L7, Canada; chowdhms@mcmaster.ca (M.C.); gfox@mcmaster.ca (G.S.F.R.); veldhu@mcmaster.ca (S.C.V.)
3 Kennametal Shared Services Gmbh, Altweiherstr 27-31, Ebermannstadt 91320, Germany; Joern.Kohlscheen@kennametal.com
* Correspondence: j.l.endrino@cranfield.ac.uk; Tel.: +44-1234-75-2931

Received: 19 August 2017; Accepted: 13 September 2017; Published: 16 September 2017

Abstract: Combinatorial deposition, comprising filtered cathodic vacuum arc (FCVA) and physical vapor deposition (PVD) magnetron sputtering is employed to deposit molybdenum disulphide (MoS_2) and titanium (Ti) thin films onto TiB_2-coated tool inserts specifically designed for the dry machining of aluminium alloys. Titanium is deposited by FCVA while MoS_2 is magnetron sputtered. The deposition set up allows several compositions of Ti-MoS_2 to be deposited simultaneously, with Ti content ranging between 5 and 96 at. %, and their machining performances to be evaluated. Milling took place using a CNC Vertical Machining Center at a 877 mm/min feed rate. The effect of different coating compositional ratios on the degree of aluminium sticking when a milling insert is used to face mill an Al alloy (SAE 6061) was investigated using a combination of energy-dispersive X-ray spectroscopy (EDX) and X-ray photoelectron spectroscopy (XPS) analysis. XPS studies suggest that the greater degree of Al sticking on the rake face of the inserts is due to the formation of greater amounts of non-protective Ti-O phases. EDX mapping of the milling inserts after machining reveal that a Ti:MoS_2 ratio of around 0.39 prevents Al from sticking to the tool edges. Since we prevent Al from sticking to the tool surface, the resultant machined surface finish is improved thus validating the machining performance of TiB_2-coated tools using optimum compositions of Ti:MoS_2 thin film coatings.

Keywords: self-lubricating composites; molybdenum disulphide; SEM; EDS; XPS; milling; aluminium

1. Introduction

Liquid lubricants have been employed as sources of lubrication in machining applications for many years [1–3]. Their main purpose is to reduce the frictional heat of the tool and suppress contact pressure [4]. Lubricants also help to remove cutting chips from the cutting area as well as removing heat during machining [5]. However, the drawbacks with lubricants are the high costs associated with their purchase as well as the costs of refrigeration and recycling [6]. Refrigeration costs can be almost four times their purchasing costs since most lubricants are not bio-degradable [7]. Hence, of importance in modern cutting applications is the search for alternatives which either minimize or avoid the production of environmentally aggressive liquid residues [8]. Dry machining is emerging as a "greener" alternative, eliminating the need for any liquid-based lubricants [9]. Although considered environmentally friendly, its main drawback is the significant impact it has on tool lifetimes due to the lack of fluid to lubricate the tool-chip area and remove heat from the cutting region [10]. Furthermore, dry machining is a serious challenge for lightweight alloys such as aluminium which during machining exhibit a high degree of plasticity [11]. The higher temperatures during machining

facilitates aluminium adhesion to the cutting tool forming a built-up edge (BUE) [12]. When the machined material adheres to the cutting edge of the tool, it changes the geometry of the cutting edge which increases the cutting forces at the tool interface [13]. The size of the BUE increases until some critical size after which it becomes unstable, with the resulting fractured particles being carried into both the chip and new workpiece surface [14]. A the result the machined part surface is rough and tool lifetime is reduced [7,13].

Existing cutting tools in dry machining applications are coated to increase their hardness, prevent the tool material from being exposed and reduce friction coefficients [5,7]. A commonly employed solid lubricant coating is molybdenum disulfide (MoS_2), which significantly improves the tribological properties of cutting tools [15], and is also typically employed in many other applications such as precision bearings, release mechanisms and space applications [16] due to its inherent low friction attributes. The characteristics of MoS_2 arise from its layered anisotropic crystal structure [17] where weak bonding between the slip planes allows atoms to slip one over another, producing the low friction coefficients observed. However, the friction coefficients degrade over time in the presence of water and oxygen due to the formation of MoO_3 [18], due to the oxidation and blistering of the topmost layers. Blistering can be prevented by co-depositing MoS_2 with a metal [19], which affects not only friction coefficients but lead to higher hardness values and lower wear resistance, not only in the presence of oxygen, but also in high humidity [18]. However the hardness, wear resistance and the lifetime of a coating in a humid environment has yet to be resolved [20].

Currently, cemented carbide mill inserts coated with TiB_2 offer the possibility of dry machining a large variety of structural metallic alloys. TiB_2 has a high hardness (~30 GPa) and excellent wear characteristics, but its brittleness and adhesion to the workpiece can sometimes prevent tool longevity [21]. In this study, hardness and the low friction coefficient of thin films of Ti and MoS_2 was studied by the deposition of a thin (200 nm) Ti:MoS_2 lubricant coating layer on TiB_2 precoated cemented carbides. A combinatorial deposition method comprising a filter cathodic arc deposition of titanium and sputtered deposition of MoS_2 was used. The use of a combinatorial deposition method offers manufacturing flexibility, increasing the speed of sample production under the same process conditions by ensuring that only the influence of the chemical composition is investigated [22,23]. Thus, the specific objectives of this study are to ascertain the degree of combinatorial control offered by FCVA and sputtering, optimising the metal-solid lubricant ratio, in an attempt to prevent aluminum sticking to the tool rake of a mill insert used to dry-machine a SAE 6061 Al alloy. The full cutting tool life evaluation is outside the scope of this article.

2. Materials and Methods

2.1. Deposition Parameters

The tungsten carbide mill inserts were as-received with 2 μm of titanium diboride (TiB_2) (Figure 1) which were DC magnetron sputtered using TiB_2 ceramic tiles on a copper back plate. Ti-MoS_2 coatings were deposited by combining magnetron sputtering (MS) with filtered cathodic vacuum arc (FCVA) techniques. Prior to deposition, the tool inserts were ultrasonically cleaned in an acetone bath for 15 min and then rinsed in isopropyl alcohol. The system base pressure was below 0.25×10^{-3} Pa prior to coating, while the system process pressure was set at 1.6 Pa. Substrates were grounded during the deposition. A range of compositions were deposited by placing a sample holder equidistant to both the Ti (FCVA) and MoS_2 (MS) sources. Substrates closer to the MoS_2 source should produce coatings with a higher MoS_2 content contrary to those placed close to the Ti source which should have higher Ti content. Figure 2 presents a schematic of the system. Ti was deposited by FCVA using a conical shaped cathode (67 mm × 50 mm × 50 mm), with the arc current set to 65 A. To prevent macro particles in the coatings the plasma was filtered using a linear filter as shown in Figure 2. The filtering coil current was set to a maximum current of 10 A. MoS_2 was sputtered from a 3-inch diameter target. Coatings were produced by simultaneously operating both the Ti and MoS_2 sources. Simultaneous deposition

on silicon allowed for step and roughness measurements of the mixed coating surfaces. Ion current measurements at the sample surface were made by connecting wires at each sample position a–e which will allow a better understanding of the influence the ion characteristics have on coating properties. Measurements at each position were collected simultaneously for 60 s, using laboratory potentiostat connected to a computer sampling at 5 Hz.

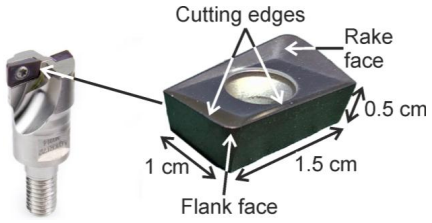

Figure 1. Widia® mill insert dimensions and its position in the milling holder [24].

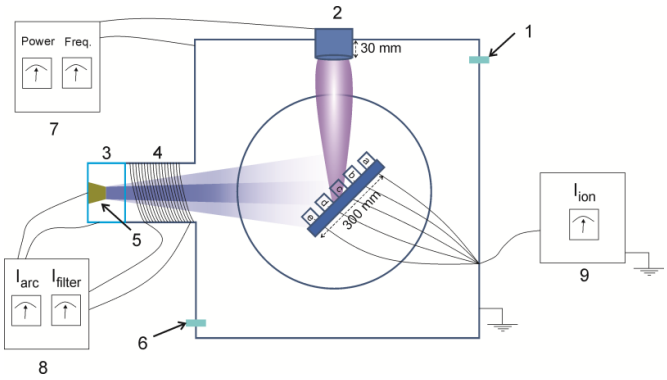

Figure 2. Top view of the chamber presenting location of the substrates (1—vacuum cryo pump inlet, 2—3" MoS_2 sputtering target, 3—anode, 4—linear filter, 5—Ti cathode, 6—argon inlet, 7—physical vapor deposition (PVD) sputtering power unit, 8—cathodic arc power unit, 9—Ametek VersaStat 4 Potentiostat).

2.2. Tribological Tests

To allow thickness measurements, a small portion of the silicon sample was covered before deposition. The difference in step between the coated and uncoated portion of the silicon was measured by a Dektak® stylus profilometer (Veeco, Cambridge, UK). The same device allowed roughness measurements to be made. Tribological tests were conducted using a ST-3001 Tribo Tester (Teer Coatings Limited, Droitwich, UK). In this test an indenter is drawn over a specimen surface with a linearly increasing load until well-defined failure occurs at critical load L_c [25]. Normal force (F_z) and tangential force (F_x) are recorded. The coefficient of friction was measured using a fixed chrome steel 5 mm-diameter ball, applying an increasing progressive load from 5 to 100 N, at a loading rate of 50 N/min and linear velocity equal to 5 mm/min. To simulate tool wear during the Al alloy machining additional tribological test were conducted using the same parameters but with Al ball.

2.3. Aluminium Milling Performance and Characterisation Tests

Face milling experiments were conducted using an Okuma Cadet Mate CNC vertical machining centre. The coated inserts were assembled on a face milling cutter with Ø 75 mm and five-flutes. The coated mill inserts were used to cut an Al alloy, SAE6061 material. The machining volume was 104,400 mm^3. The detailed cutting conditions are presented Table 1. These cutting parameters were selected according to parameters that are widely used in industry of automotive components manufacturing, such as cylinder head and engine block for semi finishing operations. Semi finish operations during cutting process reflects extreme frictions conditions for cutting tools.

Table 1. Cutting conditions.

Machine Tool	CNC Vertical Machining Centre
Tool speed [RPM]	5827
Feed rate [mm/min]	877
Feed per revolution [mm/rev]	0.15
Depth of cut [mm]	1
Total cutting length [mm]	1800
Workpiece material	Al alloy SAE 6061

The surface of the worn inserts and the scratches formed during the tribological tests were examined by scanning electron microscopy (SEM) in secondary electron mode operating at 20.0 kV. Coating composition and element mapping images were determined by using energy-dispersive X-ray spectroscopy (EDX). X-ray photoelectron spectroscopy (XPS) measurements were employed to evaluate the chemical bonding in the coatings.

The structure and any phase transformation at the cutting tool/workpiece interface, along with the chemical composition of the tribo-films, were studied by X-ray photoelectron spectroscopy (XPS) equipped with a hemispherical energy analyzer, an Al anode source for X-ray generation and a quartz crystal monochromator for focusing the generated X-rays. A monochromatic Al Kα X-ray (1486.7 eV) source was operated at 50 W–15 kV. The system base pressure was no higher than 1.0×10^{-9} Torr with an operating pressure that did not exceed 2.0×10^{-8} Torr. Before collecting any spectra, the samples were sputter-cleaned for 4 min using a 4 kV Ar^+ beam. A pass energy of 280 eV was used to obtain all survey spectra while a pass energy of 69 eV was used to collect all high-resolution data. All spectra were obtained at a 45° take off angle and a dual beam charge compensation system employed to ensure neutralization of all samples. The instrument was calibrated using a freshly cleaned Ag reference foil, where the Ag $3d_{5/2}$ peak was set to 368 eV. All data analysis was performed by computer software.

3. Results and Discussion

3.1. Combinatorial Effects

3.1.1. Ion Current Measurement

The combinatorial deposition method allows the rapid development of a range of coatings with different chemical compositions [26]. The plasma glow discharge during magnetron sputtering produces material sputtered from the surface of the target (mainly focused around the circular magnetron track) [27], in contrast to the FCVA process where the plasma is focused over a much smaller area typically referred to as cathode spots [28]. FCVA studies propose that in the absence of a magnetic field, the FCVA plasma exhibits a quadratic drop in density of particles from the spot centre [29,30]. Hence, the combination of a plasma from these two sources produces Ar^+ ions, metal Mo and S atom and FCVA Ti^+ ions colliding in complex elastic collisions in a variety of intensities depending on the distance from the source. In the case neutral-electron collision the energy transferred to the neutral from electron is very small [31]. However, if the frequency of the collisions is large then collective effect of all these collisions might be significant. On the other hand neutral-ion collisions results in charge-exchange producing fast neutral and slow ion [31]. For the large number of collisions the neutral density in the plasma centre can be depleted significantly [31]. In order to gather some insight, the variations in ion current from the physical vapor deposition (PVD) and FCVA sources were collected during deposition (Figure 3a). The current was averaged for each sample position and measured for 60 s at each individual source and with both sources started. There was little or no variation in the measured ion current when only the PVD MS source was in operation. This is due to the stability of the glow discharge typical for MS producing species with similar energies generated [32]. On the contrary, arc discharge plasmas produce ions more dynamically over the entire surface of the cathode. This produces ions with variable charge states: Ti^{1+}, Ti^{2+}, Ti^{3+}, Ti^{4+} and its

distribution [33]. E. M. Oks. et al. [33] found that for their arc ion source the distribution of the ion states was: 5% Ti^{1+}, 35% Ti^{2+}, 54% Ti^{3+} and 6% Ti^{4+}. That is reflected in the greater differences in the ion currents measured in this experiment. As expected, the currents generated from the FCVA ions are greater than the ions from PVD sputtering [28]. For MoS_2 the highest average current can be found at sample position labelled b, falling gradually with increasing distance from the MoS_2 target. However, when only the FVCA source is operational, for Ti, the highest currents were found on the sample positions a, b, and e, which indicates the tendency of the ionised plasma to expand towards the chamber walls once it is away from the linear magnetic filter [30]. Other factors influencing the spread of the plasma plume generated by FCVA include pressure gradients, shape and the size of the anode, the concentration of neutrals and external magnetic flux present in the chamber [28,34]. As the magnetron includes permanent magnets the magnetic field from them might have affected plasma expansion and ion charge [33]. In case of combinatorial deposition FCVA was found to dominate the deposition rate as the Ti-MoS_2 graph shape matches the shape of the Ti graph (Figure 3a). However, it is worth noting that the average current for samples a and b located the closest to the MoS_2 source drops when both sources are running. Interactions between neutrals and ions in this region near the MS source could result in high intensity collisions between the Ar^+ and Ti ions and neutrals resulting in some of the ionized Ti ions losing their energy due to charge-exchange with neutrals in the region near samples a and b when the MS source is running. After collision the fast neutrals are able to escape from the plasma centre [31]. This would also explain the increase in ion currents in samples d and e.

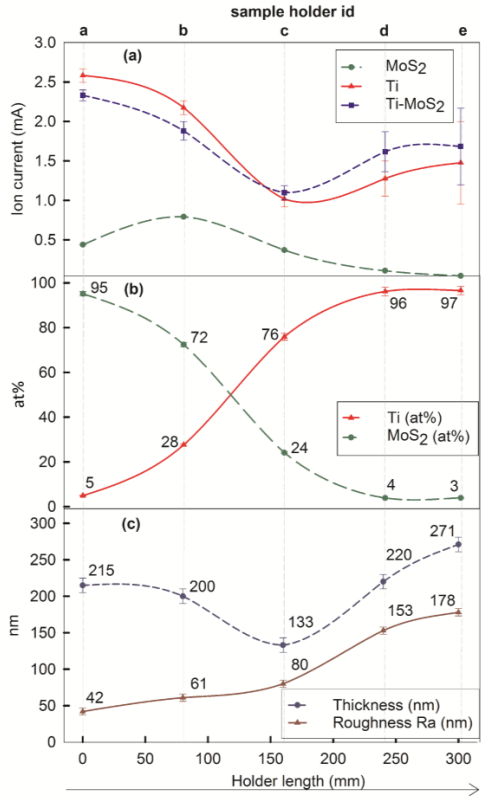

Figure 3. (**a**) Ion current measured on each of the five samples (a–e) during deposition from magnetron sputtering (MS) and filtered cathodic vacuum arc (FCVA) separately, as well as during combinatorial deposition. Each measurement made for 60 s with 5 Hz sampling speed. (**b**) Ti and Mo contents (at. %) in Ti-MoS_2 coatings on five samples (a–e). Measurements obtained by energy-dispersive X-ray spectroscopy (EDX) mode of scanning electron microscopy (SEM). (**c**) Roughness and thickness for the five samples (a–e) deposited with Ti-MoS_2 coating. Measurements done on silicon slides using Dektak® profilometer.

3.1.2. Chemical Composition

Research studies show that the greatest tribological properties have MoS_x compositions at S to Mo ratio of around 2 [35–38] as the chemical composition of thin films of MoS_2 are significantly affected by the substrate bias voltage and working pressure during deposition [39], which in turn affects the tribological and oxidation characteristics [35]. Oxygen atoms are smaller than sulphur atoms, therefore, they can easily substitute in any sites deficient in sulphur forming Mo-O-S, leading to degradation of tribological properties of MoS_2 films in air [36]. The co-deposition with Ti prevents MoS_2 degradation as Ti goes into interstitial or substitutional sites in MoS_2 and act as barrier for oxygen diffusion, thereby stabilising MoS_2 [38]. The chemical composition as a function of the sample position of the as-deposited coatings is shown in Figure 3b. Given the 200 nm thickness of these films, the EDX-SEM technique was used to quantify the Ti and MoS_2 contents in the samples. Figure 3b shows that the Ti content in the coatings increases relative to the position with the cathodic arc source. In fact, the measured chemical compositional variations follow the changes in measured ion currents. For samples at positions a and b, are dominated by the plasma from the MoS_2 source, while the samples at positions c, d and e have higher Ti contents. Moreover, samples at positions d and e seem to be more influenced by the short distance to the source (similar composition ~96 at. % Ti) than the samples positioned at both a and b. Position c, being equidistant from both MoS_2 and Ti sources, the Ti content in this sample is 3 times, greater than the Mo content. This is attributed to the greater deposition rate of the cathodic arc source compared to magnetron sputtering [40].

3.1.3. Thickness and Roughness

Figure 3c shows the thickness and roughness values for all the samples deposited. The lowest thickness value (135 nm) was measured for the sample c positioned equidistant to the MS and FVCA sources, which was also the sample with the lowest measured ion current. There are also notable differences in the thicknesses between samples d and e despite having similar compositions. This difference is likely due to the proximity of position e to the FCVA source, since the plasma density is greater in the vicinity of the front of the cathode. In fact, the ion current profile across the holder follows to great extent the measured profile thickness. During deposition, besides the charged ionized plasma from the FCVA source, macroparticles of molten cathode material created at the cathode surface [28] could pass through the linear filter and adhere to the substrate, and in some cases could decrease the density and adhesion which is undesired as it decreases the lifetime of the coating [41]. Figure 3c shows that the Ra increases with increased proximity to the Ti target. The maximum roughness of 178 nm was found for sample e, which is furthest from the MoS_2 target, and has an R_a that is almost 5 times greater than sample a. This shows a direct correlation between the deposition technique and the roughness values of the deposited sample.

3.1.4. Frictional Properties

Figure 4 shows the ball-on-flat frictional tests for the 5 deposited samples as a function of increasing load. For loads above 50 N, a coefficient of friction (CoF) ranging from 0.07 to 0.15 was obtained. The measured values are similar to other studies for MoST coatings [42]. For hybrid MoS_2/Ti coatings deposited using combined dc sputtered by high power impulse magnetron sputtering (HiPIMS) methods the reported CoF values between 0.05 and 0.23 depending on Ti content [43]. In the present study, the lowest CoF (equal to 0.07) was obtained for the sample at position b having a Ti content of around 28 at. %, in good accordance with other reported values on samples with comparable chemical composition[35]. In fact, it is worth noting that the CoF for this composition also had only little variation during ball on flat test independently of the load. The low CoF for this particular chemical composition has been related to the formation of thin MoS_2 lamellas with good adhesion to the hard titanium phase present in these coatings [38]. In this line, other research studies [37,38] concluded that the Ti to MoS_2 ratio has to be optimised for certain applications, as

too high Ti content may lower the tribological properties due to segregation of metallic titanium [37], while too low Ti content will also result in degradation of tribological properties over time due to oxidation of MoS_2 [35]. Optical microscope studies (Figure 5) of the scratches support these findings. Coatings with high (98 at. %) Ti contents (samples d and e), did not provide sufficient lubricating properties, therefore, material transferred from the ball can be observed. The wear track on sample a reveals coating failure at the start of the scratch occurs due to high MoS_2 content which is soft, and therefore fails easily under load [35]. In contrast, on the coating on sample b only little delamination can be observed for loads above 80 N, confirming the scratch test results observed in Figure 4 and proves this chemical composition of the coating can successfully prevent aluminium sticking to the tool during Al alloy machining.

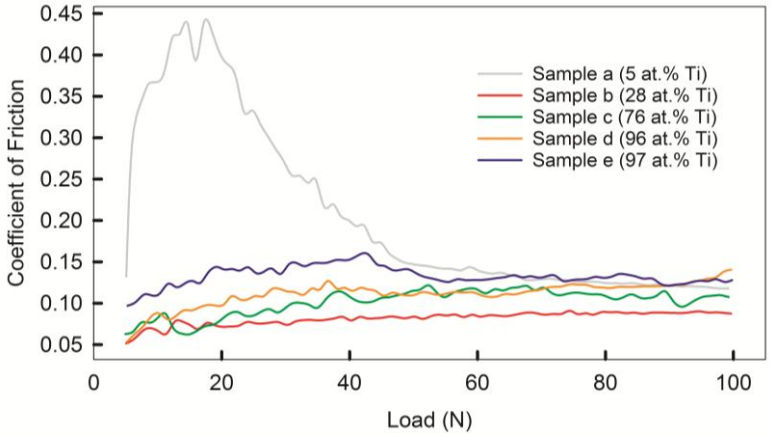

Figure 4. Friction coefficient vs. load applied for Ti-MoS_2 coatings on five samples (a–e). Tests conducted by scratch test using fixed chrome steel ball with 5 mm diameter ball sliding against a coated sample. Progressive load 5–100 N applied with 50 N/mm loading rate.

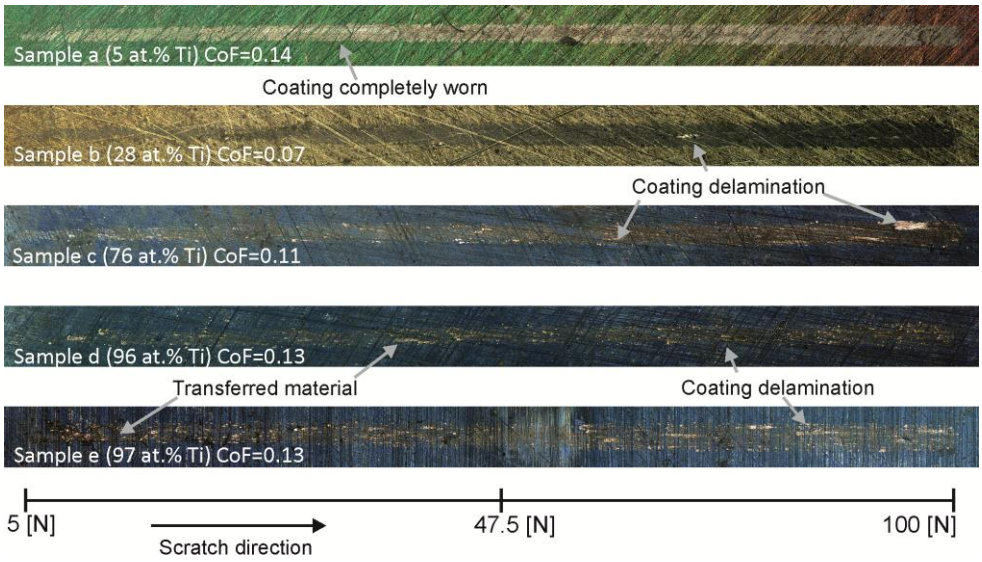

Figure 5. Optical microscope images of scratches after ball on flat frictional test with Cr ball for progressive increasing load 5–100 N.

3.2. Machining Results

Cutting tests were performed under the conditions specified in Table 1. Total length of cut was 1800 mm. The tools showed no flank wear. After that test was continued up to length of cut of 3600 mm and still no visible flank wear of the tool was observed during optical microscope studies.

3.2.1. EDX Element Mapping

EDX mapping was conducted to ascertain an optimum Ti-MoS_2 ratio which prevented Al sticking to the rake face after dry-machining an Al alloy. The bright areas in Figure 6 correspond to Al adhesion sticking to the tool rake face. No signs of Al are observed on sample b. Sample a, having 5 at. % Ti and sample c 76 at. %, has no aluminium adhering to the tool edge, however, a thin layer of aluminium can be observed on the rake face. It suggests that the composition of sample b is the optimum to prevent Al sticking to the tool rake face as it keeps the best balance between low CoF of the MoS_2 and oxidation protection of provided by Ti which could act as barriers for oxygen diffusion [38]. As there is no material adhered to the sample b the surface finish of the machined part as well as tool lifetime would be improved comparing with other samples where BUE is present [13,14]. The worst performance was indicated by samples d and e both having almost the same composition—around 96 at. % Ti. Bulk Ti does not have lubricating properties therefore coatings on sample d and e could not provide any sufficient protection against aluminium sticking [35].

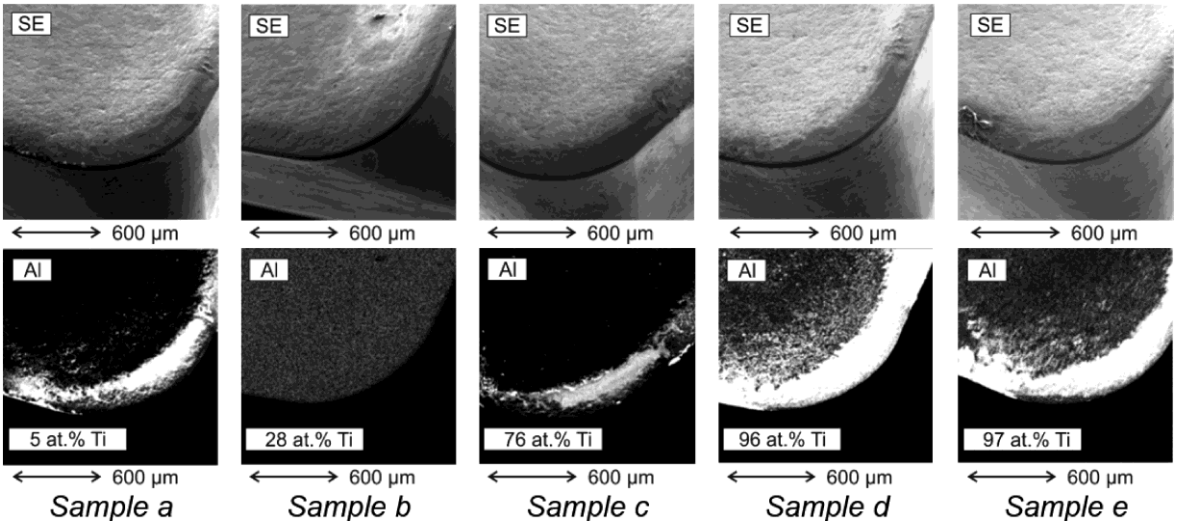

Figure 6. Aluminium element mapping images of flank face of mill inserts with Ti-MoS_2 coating after turning of 1800 mm. Element mapping obtained with EDX mode of SEM.

Similar results were obtained after the length of cut of 3600 mm (double length of cut). This indicates good tool life of the coated tool. The only difference observed between different coatings was the intensity of rake wear due to build up edge formation.

3.2.2. XPS Analysis

Samples b and c were chosen for XPS analysis as having the most contrasting chemical composition, to investigate chemical bonding of tribofilms and how it impacts on the degree of sticking of the workpiece material to the rake surface. An analysis of the phases formed during the running-in stage can be used to determine the differences in performances (protection against aluminium sticking) of the samples b and c. The B 1s, Ti 2p and Mo 3d peaks associated with B, Ti and Mo were fitted using a Gaussian-Lorentzian function as shown in Figure 6. To allow a direct comparison between

the results, the percentage atomic concentrations have been calculated by representing the ratio of the intensity to the total intensity of the electrons of the measurement.

Figure 7e,f shows that the amount of MoO_2 is greater in sample c compared with sample b. Mo-O_2 is highly undesired as it decreases lubricating properties due to volume mismatch between MoO_3 and MoS_2, which leads to disintegration of MoS_2 blisters [18]. However, in Figure 7a,b higher amounts (8.2%) of B_2O_3 can be observed in sample b. B_2O_3 is known as a solid-lubricant, having similar lamellar structure to the graphite and MoS_2 [44,45], which is the reason why it is believed this particular composition offered the best performance in terms of preventing Al sticking to the rake face. Ti_2O_3 has doublet binding energy at 457.2 and 462.2 in sample b. As can be seen in Figure 7c,d, sample c has greater degree of TiO bonding compared to sample b and therefore, forms a greater TiO tribo-oxide layer which is believed to be the main reason of poorer wear resistance in Ti-based alloys. It is considered that this tribo-oxide is not adherent to the substrate, is also brittle and tends to be fragmented, and therefore does not have any protective role during machining [46,47]. Although, at temperatures above 600 °C tribo-oxides can play a protective role [46], since machining in this study was performed at temparatures below 300 °C, it is most probably the formation of greater amounts of Ti-O tribo-phase in sample c causes a poor wear performance (more intensive sticking of Al on the rake face) than found in sample b.

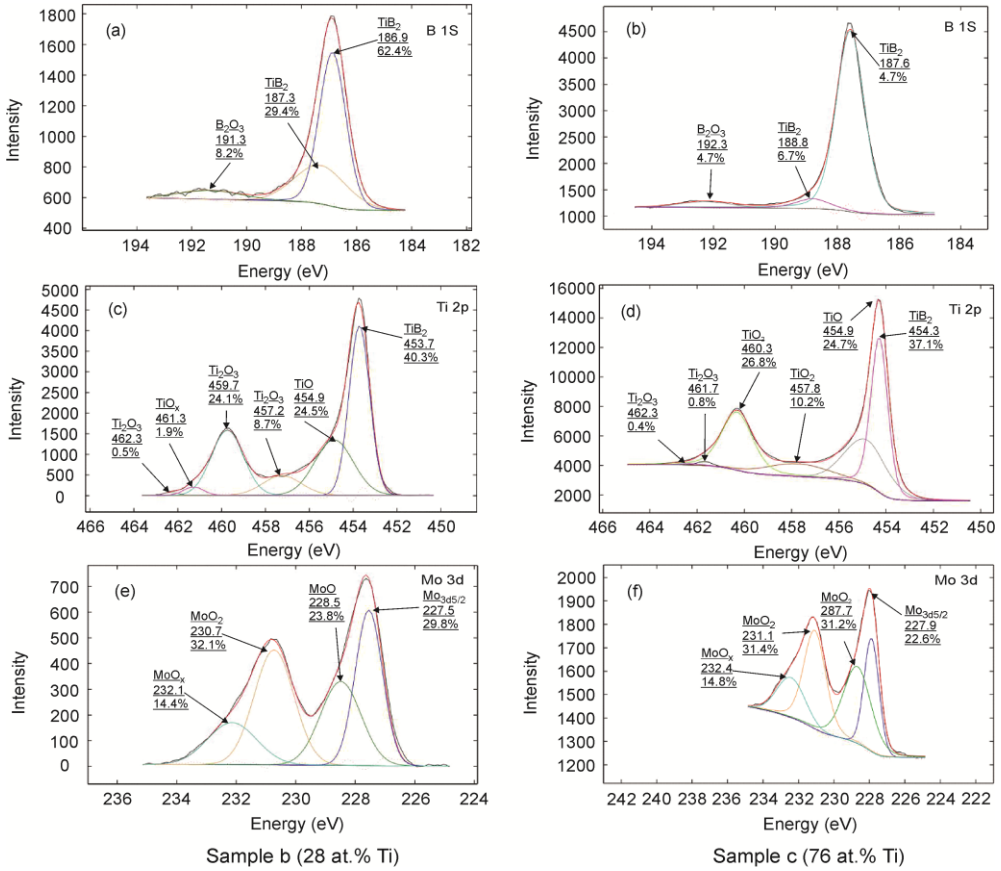

Figure 7. Sample b (**a**,**c**,**e**) and sample c (**b**,**d**,**f**) photoelectron spectra of (**a**,**b**) B 1s, (**c**,**d**) Ti 2p and (**e**,**f**) Mo 3d on rake face after total 1800 mm of milling.

3.3. Ball-on-Flat Frictional Test

To support the results from the milling tests a series of ball-on-flat frictional tests were performed on all samples using Al balls. The degree of Al transferred to the insert was determined using optical microscope. The slightly lighter areas in Figure 8 correspond to a transfer layer of Al within the wear

track. Comparing to other samples large amount of Al transferred to the insert can be found on sample a for a lower loads (<50 N). This can be attributed to a high content of soft MoS_2 in this coating, as a consequence the coating debris accumulating in front of the ball becomes entrapped and serves as a self-lubricating layer at higher loads. There was little or no Al transferred observed for sample b over the entire range of loads, and the Al transferred from the ball is present in the form of small discontinuous "clumps". These observations support the findings that the composition of the sample b is the optimum to prevent Al sticking during Al-alloy machining. Compare and contrast this with samples d and e containing a high amount of Ti, where a large amount of Al can be found for both compositions, proving poor protection against Al sticking of Ti.

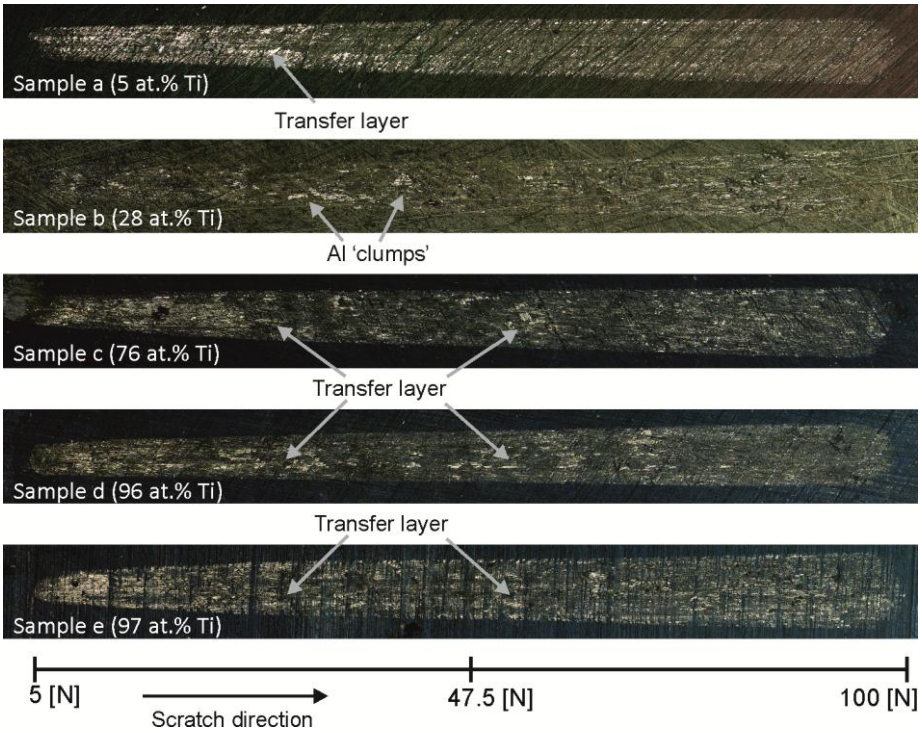

Figure 8. Optical microscope images of scratches after ball on flat frictional test with an Al ball, for progressive increasing load 5–100 N.

4. Conclusions

A hybrid filtered vacuum cathodic arc-magnetron sputtering system was successfully used to deposit composite Ti-MoS_2 on five TiB_2-coated milling inserts with Ti contents ranging from 5 to 97 at. %, which varied according to the distance from both Ti and MoS_2 sources. Tool inserts placed close to Ti source produced at. % Ti higher to those placed close to MoS_2 that had mixture of Ti and MoS_2 contents. Ion current measurements revealed that FCVA dominated the deposition rate though the plasma expansion towards the chamber walls. Interactions between neutrals from MS and ions from FCVA led to the lowest ion current being measured on the sample placed equidistant from both Ti and MoS_2 sources. There is a correlation between the changes measured in the ion current during deposition and variations in thickness, which increased with increasing titanium content. The roughness increased with increasing proximity to FCVA source due in part to the influence of unfiltered macroparticles during deposition, correlating with large variations ion currents measured on samples placed the closest to the Ti source. Combinatorial deposition of Ti with MoS_2 led to reduced frictional properties of inserts with Ti:MoS_2 ratios between 0.05 and 3. Ball-on-flat frictional tests, EDX mapping and aluminium alloy face milling machining tests indicated that a coating with around 28 at. % of Ti had the lowest friction coefficient 0.07 for loads between 40 and 100 N. This particular

composition successfully prevented aluminium sticking to the rake of the tool after cutting at a length of 3.6 m. This result was confirmed after ball on flat frictional test with aluminium ball for 20 N load, as only a little Al was found to be adherent to the scratch. XPS studies revealed greater sticking of Al on the rake face with different Ti:MoS_2 ratios, and is likely caused by the formation of slightly higher amounts of non-protective Ti-O phase. Overall, this study demonstrates the potential of combinatorial deposition for rapid development of hard lubricant coatings.

Author Contributions: Tomasz L. Brzezinka wrote the paper, Jeff Rao and Jose L. Endrino provided research supervision and proofreading of the manuscript, Mohamad Chowdhury performed the machining, German S. Fox Rabinovich and Stephen C. Veldhuis characterized the worn inserts with EDX element mapping and XPS analysis, Joern Kohlscheen contribute to the technical aspects of the materials used.

Conflicts of Interest: The authors declare no conflict of interest.

References

1. Vereschaka, A.A.; Grigoriev, S.N.; Vereschaka, A.S.; Popov, A.Y.; Batako, A.D. Nano-scale multilayered composite coatings for cutting tools operating under heavy cutting conditions. *Procedia CIRP* **2014**, *14*, 239–244. [CrossRef]
2. Aoyama, T. Development of a mixture supply system for machining with minimal quantity lubrication. *CIRP Ann. Manuf. Technol.* **2002**, *51*, 289–292. [CrossRef]
3. Obikawa, T. Machining with least quantity lubrication. In *Comprehensive Materials Processing*; Hashmi, S., Ed.; Elsevier: Amsterdam, The Netherlands, 2014; Volume 11, pp. 255–281. ISBN 978-0-08-096533-8.
4. Itoigawa, F.; Childs, T.H.C.; Nakamura, T.; Belluco, W. Effects and mechanisms in minimal quantity lubrication machining of an aluminum alloy. *Wear* **2006**, *260*, 339–344. [CrossRef]
5. Rivero, A.; Aramendi, G.; Herranz, S.; De Lacalle, L.N.L. An experimental investigation of the effect of coatings and cutting parameters on the dry drilling performance of aluminium alloys. *Int. J. Adv. Manuf. Technol.* **2006**, *28*, 1–11. [CrossRef]
6. Braga, D.U.; Diniz, A.E.; Miranda, G.W.A.; Coppini, N.L. Using a minimum quantity of lubricant (MQL) and a diamond coated tool in the drilling of aluminum-silicon alloys. *J. Mater. Process. Technol.* **2002**, *122*, 127–138. [CrossRef]
7. Shokrani, A.; Dhokia, V.; Newman, S.T. Environmentally conscious machining of difficult-to-machine materials with regard to cutting fluids. *Int. J. Mach. Tools Manuf.* **2012**, *57*, 83–101. [CrossRef]
8. Sreejith, P.S. Machining of 6061 aluminium alloy with MQL, dry and flooded lubricant conditions. *Mater. Lett.* **2008**, *62*, 276–278. [CrossRef]
9. Fox-Rabinovich, G.; Dasch, J.M.; Wagg, T.; Yamamoto, K.; Veldhuis, S.; Dosbaeva, G.K.; Tauhiduzzaman, M. Cutting performance of different coatings during minimum quantity lubrication drilling of aluminum silicon B319 cast alloy. *Surf. Coat. Technol.* **2011**, *205*, 4107–4116. [CrossRef]
10. Hanyu, H.; Kamiya, S.; Murakami, Y.; Saka, M. Dry and semi-dry machining using finely crystallized diamond coating cutting tools. *Surf. Coat. Technol.* **2003**, *174–175*, 720–724. [CrossRef]
11. Dosbaeva, J.; Fox-Rabinovich, G.; Dasch, J.; Veldhuis, S. Enhancement of wet- and MQL-based machining of automotive alloys using cutting tools with DLC/polymer surface treatments. *J. Mater. Eng. Perform.* **2008**, *17*, 346–351. [CrossRef]
12. Bhowmick, S.; Alpas, A.T. Minimum quantity lubrication drilling of aluminium-silicon alloys in water using diamond-like carbon coated drills. *Int. J. Mach. Tools Manuf.* **2008**, *48*, 1429–1443. [CrossRef]
13. Ramaswami, R. The effect of the built-up-edge(BUE) on the wear of cutting tools. *Wear* **1971**, *18*, 1–10. [CrossRef]
14. Yang, G.-C.; Ao, S.-L.; Gelman, L. *IAENG Transactions on Engineering Technologies*; Springer: Dordrecht, The Netherlands, 2013; Volume 170, ISBN 978-9-40-074785-2.
15. Gu, L.; Ke, P.; Zou, Y.; Li, X.; Wang, A. Amorphous self-lubricant MoS_2-C sputtered coating with high hardness. *Appl. Surf. Sci.* **2015**, *331*, 66–71. [CrossRef]
16. Renevier, N.M.; Lobiondo, N.; Fox, V.C.; Teer, D.G.; Hampshire, J. Performance of MoS_2/metal composite coatings used for dry machining and other industrial applications. *Surf. Coat. Technol.* **2000**, *123*, 84–91. [CrossRef]

17. Teer, D.G.; Hampshire, J.; Fox, V.; Bellido-Gonzalez, V. The tribological properties of MoS_2/metal composite coatings deposited by closed field magnetron sputtering. *Surf. Coat. Technol.* **1997**, *94–95*, 572–577. [CrossRef]
18. Moskalewicz, T.; Zimowski, S.; Wendler, B.; Nolbrzak, P.; Czyrska-Filemonowicz, A. Microstructure and tribological properties of low-friction composite MoS_2(Ti,W) coating on the oxygen hardened Ti-6Al-4V alloy. *Met. Mater. Int.* **2014**, *20*, 269–276. [CrossRef]
19. Bhaduri, D.; Kumar, R.; Jain, A.K.; Chattopadhyay, A.K. On tribological behaviour and application of TiN and MoS_2-Ti composite coating for enhancing performance of monolayer cBN grinding wheel. *Wear* **2010**, *268*, 1053–1065. [CrossRef]
20. Simmonds, M.; Savan, A.; Van Swygenhoven, H.; Pflüger, E.; Mikhailov, S. Structural, morphological, chemical and tribological investigations of sputter deposited MoS_x/metal multilayer coatings. *Surf. Coat. Technol.* **1998**, *108–109*, 340–344. [CrossRef]
21. Rao, J.; Cruz, R.; Lawson, K.J.; Nicholls, J.R. Carbon and titanium diboride (TiB_2) multilayer coatings. *Diam. Relat. Mater.* **2004**, *13*, 2221–2225. [CrossRef]
22. Adhiprakasha, E.; Niyogi, S.; Ramani, K.; Ryan, V. Mixed-metal barrier films optimized by high-productivity combinatorial PVD. U.S. Patent 20150021772 A1, 22 January 2015.
23. Cremer, R.; Neuschütz, D. A combinatorial approach to the optimization of metastable multicomponent hard coatings. *Surf. Coat. Technol.* **2001**, *146–147*, 229–236. [CrossRef]
24. Indexable End Mill, 2 Flute, 17 mm, Center Cut, Tormach. Available online: http://lmscnc.com/4806 (accessed on 24 October 2016).
25. Bull, S.J. Failure modes in scratch adhesion testing. *Surf. Coat. Technol.* **1991**, *50*, 25–32. [CrossRef]
26. Hanak, J.J. The "multiple-sample concept" in materials research: Synthesis, compositional analysis and testing of entire multicomponent systems. *J. Mater. Sci.* **1970**, *5*, 964–971. [CrossRef]
27. Anders, A. A review comparing cathodic arcs and high power impulse magnetron sputtering (HiPIMS). *Surf. Coat. Technol.* **2014**, *257*, 308–325. [CrossRef]
28. Anders, A. *Cathodic Arcs: From Fractal Spots to Energetic Condensation*; Springer Inc.: New York, NY, USA, 2008; ISBN 978-0-38-779107-4.
29. Jütner, B. Characterization of the cathode spot. *IEEE Trans. Plasma Sci.* **1987**, *15*, 474–480. [CrossRef]
30. Ivanov, V.A.; Pursch, H. Time-resolved measurements of the parameters of arc cathode plasmas in vacuum. *IEEE Trans. Plasma Sci.* **1985**, *13*, 334–336. [CrossRef]
31. Hori, T.; Bowden, M.D.; Uchino, K.; Muraoka, K.; Maeda, M.; Hori, T.; Bowden, M.D.; Uchino, K.; Muraoka, K. Measurements of electron temperature, electron density, and neutral density in a radio frequency inductively coupled plasma measurements of electron temperature, electron density, and neutral density in a radio-frequency inductively coupled plasma. *J. Vac. Sci. Technol. A* **2014**, *144*. [CrossRef]
32. Buck, V. Structure and density of sputtered MoS_2-films. *Vacuum* **1986**, *36*, 89–94. [CrossRef]
33. Oks, E.M.; Brown, I.G.; Dickinson, M.R.; MacGill, R.A.; Emig, H.; Spädtke, P.; Wolf, B.H. Elevated ion charge states in vacuum arc plasmas in a magnetic field. *Appl. Phys. Lett.* **1995**, *67*, 200–202. [CrossRef]
34. Anders, A. The fractal nature of vacuum arc cathode spots. *IEEE Trans. Plasma Sci.* **2005**, *33*, 1456–1464. [CrossRef]
35. Arslan, E.; Bülbül, F.; Efeoglu, I. The structural and tribological properties of MoS_2-Ti composite solid lubricants. *Tribol. Trans.* **2004**, *47*, 37–41. [CrossRef]
36. Buck, V. Lattice parameters of sputtered MoS_2 films. *Thin Solid Films* **1991**, *198*, 157–167. [CrossRef]
37. Rigato, V.; Maggioni, G.; Boscarino, D.; Sangaletti, L.; Depero, L.; Fox, V.C.; Teer, D.; Santini, C. A study of the structural and mechanical properties of Ti-MoS_2 coatings deposited by closed field unbalanced magnetron sputter ion plating. *Surf. Coat. Technol.* **1999**, *116*, 176–183. [CrossRef]
38. Kim, S.K.; Ahn, Y.-H.; Kim, K.H. MoS_2-Ti composite coatings on tool steel by d.c. magnetron sputtering. *Surface Coatings Technol.* **2003**, *169–170*, 428–432.
39. Bülbül, F.; Efeoğlu, I.; Arslan, E. The effect of bias voltage and working pressure on S/Mo ratio at MoS_2-Ti composite films. *Appl. Surf. Sci.* **2007**, *253*, 4415–4419. [CrossRef]
40. Zhao, L.R.; Lupandina, O.; Pankov, V.V.; McKellar, R.C. Microstructures of NiCrAlY coating applied on CMSX-4 by cathodic arc deposition. In Proceedings of the ASME Turbo Expo 2014: Turbine Technical Conference and Expositon, Düsseldorf, Germany, 16–20 June 2014.
41. Sanders, D.M.; Anders, A. Review of cathodic arc deposition technology at the start of the new millennium. *Surf. Coat. Technol.* **2000**, *133–134*, 78–90. [CrossRef]

42. Donnet, C.; Martin, J.M.; Le Mogne, T.; Belin, M. Super-low friction coefficient of MoS_2 coatings in various environments. *Tribol. Ser.* **1994**, *27*, 277–284. [CrossRef]
43. Qin, X.; Ke, P.; Wang, A.; Kim, K.H. Microstructure, mechanical and tribological behaviors of MoS_2-Ti composite coatings deposited by a hybrid HIPIMS method. *Surf. Coat. Technol.* **2013**, *228*, 275–281. [CrossRef]
44. Burroughs, B.R.; Kim, J.-H.; Blanchet, T.A. Boric acid self-lubrication of B_2O_3—filled polymer composites. *Tribol. Trans.* **1999**, *42*, 592–600. [CrossRef]
45. Hu, Z.B.; Li, H.J.; Fu, Q.G.; Xue, H.; Sun, G.L. Fabrication and tribological properties of B_2O_3 as friction reducing coatings for carbon-carbon composites. *New Carbon Mater.* **2007**, *22*, 131–134. [CrossRef]
46. Zhang, Q.Y.; Zhou, Y.; Wang, L.; Cui, X.H.; Wang, S.Q. Investigation on tribo-layers and their function of a titanium alloy during dry sliding. *Tribol. Int.* **2016**, *94*, 541–549. [CrossRef]
47. Wang, L.; Li, X.X.; Zhou, Y.; Zhang, Q.Y.; Chen, K.M.; Wang, S.Q. Relations of counterface materials with stability of tribo-oxide layer and wear behavior of Ti–6.5Al–3.5Mo–1.5Zr–0.3Si alloy. *Tribol. Int.* **2015**, *91*, 246–257. [CrossRef]

2017-09-16

Hybrid Ti-MoS2 coatings for dry machining of aluminium alloys

Brzezinka, Tomasz L.

MDPI

Brzezinka TL, Rao J, Chowdhury M, et al., (2017) Hybrid Ti-MoS2 coatings for dry machining of aluminium alloys. Coatings, Volume 7, Issue 9, 2017, Article number 149
http://dx.doi.org/10.3390/coatings7090149